PCCP

Accepted Manuscript

This article can be cited before page numbers have been issued, to do this please use: A. Perez-Guardiola, M. E. Sandoval-Salinas, D. Casanova, E. San Fabián, Á. J. J. Pérez-Jiménez and J. Sancho-Garcia, *Phys. Chem. Chem. Phys.*, 2018, DOI: 10.1039/C8CP00135A.

This is an Accepted Manuscript, which has been through the Royal Society of Chemistry peer review process and has been accepted for publication.

Accepted Manuscripts are published online shortly after acceptance, before technical editing, formatting and proof reading. Using this free service, authors can make their results available to the community, in citable form, before we publish the edited article. We will replace this Accepted Manuscript with the edited and formatted Advance Article as soon as it is available.

You can find more information about Accepted Manuscripts in the author guidelines.

Please note that technical editing may introduce minor changes to the text and/or graphics, which may alter content. The journal's standard Terms & Conditions and the ethical guidelines, outlined in our author and reviewer resource centre, still apply. In no event shall the Royal Society of Chemistry be held responsible for any errors or omissions in this Accepted Manuscript or any consequences arising from the use of any information it contains.

ROYAL SOCIETY OF CHEMISTRY

rsc.li/pccp

View Article Online
DOI: 10.1039/C8CP00135A

The Role of Topology in Organic Molecules: Origin and Comparison of the Radical Character in Linear and Cyclic Oligoacenes and Related Oligomers

A. Pérez-Guardiola[1], M. E. Sandoval-Salinas[2,3], D. Casanova[3,4]*, E. San-Fabián[1], A. J. Pérez-Jiménez[1], and J. C. Sancho-García[1]†

[1] Department of Physical Chemistry,
University of Alicante,
E-03080 Alicante, Spain

[2] Departament de Ciéncia de Materials i Química Física,
Institut de Química Teòrica i Computacional (IQTCUB),
Universitat de Barcelona,
E-08028 Barcelona, Spain

[3] Kimika Fakultatea,
Euskal Herriko Unibertsitatea (UPV/EHU)
and Donostia International Physics Center (DIPC),
E-20018 Donostia, Spain

[4] IKERBASQUE,
Basque Foundation for Science,
E-48013 Bilbao, Spain

February 7, 2018

View Article Online
DOI: 10.1039/C8CP00135A

*E-mail: david.casanova@ehu.eus
†E-mail: jc.sancho@ua.es

View Article Online
DOI: 10.1039/C8CP00135A

Abstract

We discuss the nature of electron-correlation effects in carbon nanorings and nanobelts by the analysis tool known as fractional occupation number weighted electron density (ρ^{FOD}) and the RAS-SF method, revealing for the first time significant differences in static correlation effects depending on how the rings (i.e. chemical units) are fused and/or connected until closing the loop. We choose to study in detail linear and cyclic oligoacene molecules of increasing size, and relate the emerging differences with the difficulties for the synthesis of the latter due to their radicaloid character. We finally explore how minor structural modifications of the cyclic forms can alter these results, showing the potential use of these systems as molecular templates for the growth of well-shaped carbon nanotubes as well as the usefulness of theoretical tools for molecular design.

Key words: Oligoacenes, Cyclacenes, bi- or poly-radicals, fractional orbital occupation, FT-DFT, RAS-SF.

View Article Online
DOI: 10.1039/C8CP00135A

1 Introduction

Nowadays, there is a growing and worldwide interest for the study of cyclic organic molecules of limited size, constituted by fused or bound benzene rings,[1–8] as molecular templates (i.e. chemical precursors) for the synthesis and growth of size-specific Single-Walled Carbon NanoTubes (SWCNT), which could be afforded under certain experimental conditions still under investigation.[9] Probably the best known examples are the CycloParaPhenylene (CPP) compounds (see Figure 1) leading to SWCNT with armchair edges in this case. Other interesting family is formed by CyclaCene (CC) molecules of increasing size, see also Figure 1, which would ideally give rise to zig-zag SWCNT of controlled diameter and shape. It should be indicated that [n]CPPs are experimentally produced at the gram-scale and can be synthesized following several routes. On the other hand, many groups have historically attempted to synthesize [n]CC compounds without success,[10] whereas pristine linear acenes have been synthesized up to hexacene[11] and very recently heptacene,[12,13] and up to nonacene using stabilization strategies based on chemical substitution.[14] Furthermore, the molecule [3]cyclobenzo[a]anthracene, an isomer of [12]cyclophenacene, has been successfully synthesized,[15] recrystallized and its structure has been confirmed by X-ray data. This achievement paves the way for the production of belt-shaped compounds, constituting thus a major breakthrough possibly inspiring other discoveries soon.

The strong tendency of some of these organic compounds to react with the environment has been associated with their diradical (or polyradical) character, which for instance would explain why the stability of linear acenes decreases as the number of fused rings increases. Therefore, in order to ra-

View Article Online
DOI: 10.1039/C8CP00135A

tionally design stable nanostructures to be used as molecular building blocks for the synthesis of nanotubes, it is necessary to comprehend their electronic properties in general, and the physical origin of their diradicaloid nature in particular. From the theoretical and computational point of view, elucidating the bi- or polyradical character of organic molecules is a longstanding research effort from decades ago, whose origin can be traced back to difficulties of theoretical methods to include Strong Correlation Effects[16–20] (SCE), also called static, left-right, nondynamical, or multicenter, in a cost-effective and systematic manner. These effects often manifest into a small or even vanishing one-electron energy gap, i.e. the energy difference between frontier molecular orbitals, posing consequently a great challenge to Density Functional Theory (DFT) methods within the Kohn-Sham (KS) formulation due to its intrinsic one-determinantal nature and/or the lack of a known exact density functional.[21–24] Knowing *a priori* if a system is affected or not by SCE is not an easy task. Some global diagnostics exist in the literature like T_1/D_1[25,26] or A_λ,[27] but they are based on costly calculations which might hamper the judicious choice of single- or multi-reference electronic structure methods for large systems or for a fast screening of compounds. Note also that only very recently local descriptors of electron correlation have appeared[28] too.

Previous considerable and remarkable efforts extended the standard KS formalism to cope with these SCE, making use of the on-top pair density,[29–38] the *ensemble* of pure determinantal states,[39–41] the adequate and balanced coupling between some *ab initio* method with a density functional (e.g. DFT-MRCI,[42] CAS-DFT,[43,44] CASCI-DFT,[45] or spin-projected UHF-DFT[46,47]), the spin-flip approach,[48] the Becke'05 correlation model,[49] the spin densities

View Article Online
DOI: 10.1039/C8CP00135A

$\rho_</\rho_>$ based on natural orbitals,[50] the pair natural orbital functional theory,[51,52] the fractional-spin occupations,[53] or the recently developed Multi-configuration Pair-Density Functional Theory (MC-PDFT),[54–57] to explicitly mention just a few of them.

Interestingly, another route recently pursued circumvents these difficulties and aims at simulating SCE by fractional orbital occupations, as it may be naturally arising in the systems affected by it, thus avoiding issues as the double-counting of correlation contributions (i.e. static and dynamic) and benefiting from a more practical implementation. This kind of methods[58–60] provide fractional orbital occupations by a Fermi-Dirac distribution under the effect of a fictitious temperature θ (several thousands of K) to force that occupation, with these techniques generally referred as Finite-Temperature (FT-) DFT or Fermi-Smearing[61] and Thermally-Assisted-Occupation (TAO) DFT.[62] However, it was not until recently that this theory has been proposed to serve as an interpretative tool to predict, analyze, and thus rationalize, SCE in any chemical system,[63,64] which we would like to further exploit here for disclosing structure-property relationships of organic molecules of cyclic topology.

In the following, we will introduce the theoretical framework employed before presenting results for $[n]$CPP and $[n]$CC molecules with $n = 5 - 12$ units, the latter extensively compared with the parent linear compounds. We try next to disclose the role played by cyclic topology, and conclude presenting results for other nanobelts recently synthesized efficiently. We will compare systematically results achieved from the FT-DFT method with those from the Restricted-Active-Space (RAS) Spin-Flip (SF) method,[65] which will

View Article Online
DOI: 10.1039/C8CP00135A

allow to merge the best of both worlds, DFT and wave function based models, while achieving results of high accuracy. These two methods bring two rather different perspectives for the description of electronic systems were strong correlation might be important, and their combined use might result in an clear description of molecular systems. Moreover, the FT-DFT analysis provides a general framework for the quantification of the (poly)radicaloid character for electronic densities obtained within different methods. Overall, these results should help to find out why some nanorings are synthesized and others not, as well as displaying the usefulness of these theoretical tools for this exciting field of knowledge.

2 Theoretical framework

2.1 The FT-DFT method and the FOD analysis

In standard KS-DFT calculations, the ground-state electronic density is built upon the lowest N occupied spin-orbitals φ_i as:

$$\rho^{\mathrm{KS-DFT}}(\mathbf{r}) = \sum_{i}^{N} |\varphi_i(\mathbf{r})|^2, \tag{1}$$

with the corresponding energy levels given by ε_i. Since degeneracies do not often arise in common systems, the orbital occupation numbers are 0 or 1. Deviations from this situation are typically associated with the presence of strong electron correlations and can be rectified by the introduction of fractional occupation numbers:

$$\rho(\mathbf{r}) = \sum_{i}^{\infty} f_i |\phi_i(\mathbf{r})|^2, \tag{2}$$

employing hereby a finite-temperature DFT approach with f_i the fractional occupation numbers ($0 \leq f_i \leq 1$) of a new set of orbitals ϕ_i. These orbitals

View Article Online
DOI: 10.1039/C8CP00135A

are self-consistently obtained by minimizing the Gibbs electronic free energy ($G_{el} = E_{el} - T_{el}S_{el}$) of the system at a fictitious pseudo-temperature (i.e. electronic) called T_{el}. The fractional occupation numbers f_i are determined from the Fermi-Dirac distribution:

$$f_i = \frac{1}{1 + e^{(\epsilon_i - E_F)/\theta}}, \tag{3}$$

depending critically on the $\epsilon_i - E_F$ difference and on $\theta = k_B T_{el}$, which actually depends on the exchange-correlation functional used for these calculations. Under this approach, it is possible to define a Fractional Orbital Density (FOD) as an analysis tool of static correlation:[63,64]

$$\rho^{\mathrm{FOD}}(\mathbf{r}) = \sum_{i}^{M} (\delta_1 - \delta_2 f_i) \, |\phi_i(\mathbf{r})|^2, \tag{4}$$

where ideally $M \to \infty$ and is the dimension of the finite basis set in practice, δ_1 and δ_2 are chosen to become $(1, 1)$ if the single-particle energy level (ϵ_i) is lower than the energy of the Fermi level, E_F, or $(0, -1)$ otherwise. Representation of natural orbitals with fractional occupations and/or the associated electron density, i.e. ρ^{FOD}, has repeatedly shown to be a very useful and intuitive computational tool to understand the distributions of unpaired elenctrons in molecular systems.[66–68] Note finally that the integral of $\rho^{\mathrm{FOD}}(\mathbf{r})$ over all the spatial space yields the highly useful N_{FOD} value, that is, an estimation of the number of strongly correlated electrons. The S_{el} entropy, connected with the symmetrized von Neumann entropy, is related with the entanglement of electronic states and may be also obtained from the corresponding f_i values, as explained and shown in the Supporting Information.

View Article Online
DOI: 10.1039/C8CP00135A

2.2 The RAS-SF method

Within the realm of wave function approaches able to deal with degeneracies or near-degeneracies, Spin-Flip (SF) methods have shown to be a reliable approach in many cases.[69,70] In particular, the definition of a Restricted Active Space (RAS) in conjunction with a SF excitation operator (promotion of α electrons into empty β orbitals), i.e. the RAS-SF method, represents a balanced and computationally affordable approach to the study of molecular systems with radical or polyradical character. One of the typical metrics employed to evaluate the amount of polyradicalism of RAS-SF electronic states is through the expression introduced by Head-Gordon,[71] to quantify the number of unpaired electrons:

$$N_U = \sum_i \left(1 - \mathrm{abs}\left(1 - n_i\right)\right), \tag{5}$$

where $\{n_i\}$ are the electron occupancies of the RAS-SF natural orbitals ($0 \leq n_i \leq 2$). Close inspection of Eqs. (4) and (5) reveals the equivalence of N_U and the integration of ρ^{FOD} (N_{FOD}). Therefore, in the following we will exclusively use the N_{FOD} label to quantify the number of unpaired electrons of electronic states computed with both approaches, i.e. FT-DFT and RAS-SF. Figure S1 shows the correlation between both approaches applied to the case of oligoacenes.

3 Computational details

The geometries of the compounds were optimized at the (restricted) M06-2X/6-31+G* level, using the Gaussian09 package[72] and the ultrafine grid, and their nature confirmed as global minima by the corresponding all-real vibrational frequencies. The use of a broken-symmetry guess to optimize the

View Article Online
DOI: 10.1039/C8CP00135A

ground-state geometry of the molecules did not appreciably alter any of the results exposed here. The choice of the M06-2X functional[73] is motivated by a previous study showing that this method provides sufficiently accurate structures for cyclic nanorings compared with the long-range dispersion-corrected M06-2X-D3(BJ) extension.[74] Then, the FT-DFT calculations were done at the (unrestricted) TPSS/def2-TZVP level using the ORCA 4.0.0.2 package[75] with the default temperature T_{el} = 5000K as originally recommended for this functional. The isocontour values for the FOD plots were set to 0.005 e/bohr^3, except for borderline cases for which a value of 0.002 e/bohr^3 is instead fixed to better appreciate the corresponding isosurfaces. The FOD plots were generated with UCSF Chimera[76] (version 1.12).

The RAS-SF calculations were done with a development version of the Q-Chem program[77] and with the 6-31G(d) basis set. RAS-SF calculations used the lowest ROHF (Restricted Open-Shell) triplet state as a reference configuration in all the systems but the cyclic acenes with an odd number of rings, for which the lowest ROHF quintet orbitals were employed instead. The restricted orbital space considered 8 electrons in 8 π-orbitals for the RAS2 subspace, as recently recommended for CASSCF, and all virtuals and doubly occupied π-orbitals for the RAS1 and RAS3 subspaces, respectively. Excitations from core electrons (1s C orbitals) were disregarded. Fragment decomposition of the RAS-SF ground state function of even [n]CC molecules have been done considering a RAS2 subspace with 2 electrons in 2 π-orbitals. Molecular orbital energies for the Hückel model were obtained with $\alpha < 0$, $\beta = \alpha/10$ and $\gamma = \beta/5$ for the Coulomb and resonance integrals.

View Article Online
DOI: 10.1039/C8CP00135A

4 Results and discussion

4.1 Cycloparaphenylenes

A relatively large number of cycloparahenylenes have been synthesized efficiently and following different routes since 2008, as said before, with multiple possibilities for cutting-edge applications such as: (i) self-aggregation to form stable molecular crystals[78] with specific porosity arising from well-defined microscopic orientations,[79] (ii) nanocontainers for encapsulating pristine or fine-tuned fullerenes,[80–82] and (iii) creation of (sub)-nanochannels or tweezers of controlled length and/or chirality[83] after dimerization. These applications thus showing their versatile chemical character and some of their nanofunctions. The FOD plots (not shown here) for the set of the [n]CPPs studied, with $n = 5 - 12$, become visible only for a cut-off of 0.002 e/bohr^3, indicating thus a minor polyradicaloid nature as it was expected from their allowed synthesis and applications, which may be also seen as a proof of concept. The corresponding N_{FOD} values (Table S1) for all the studied compounds are comprised between 0.467 and 0.636 and thus admittedly low, although slightly increasing with the system size. Actually, from these results and its comparison with standard molecules,[63] it can be inferred a negligible presence of SCE in agreement with their afforded synthesis by many groups and in different conditions.

4.2 Linear and cyclic oligoacenes

4.2.1 Generalities

We analyze and compare next linear and cyclic oligoacenes of increasing size, noticing that some of the FT-TPSS results for the odd-numbered linear systems (i.e. anthracene, pentacene, and heptacene) were also included

View Article Online
DOI: 10.1039/C8CP00135A

in previous publications[63,64] although not compared with the parent cyclic forms neither with RAS-SF results. According to the Clar's sextet rule long acenes tend to be rather reactive since only one aromatic sextet ring can be drawn for resonance structures with no radical centers (see Figure S2 in the Supporting Information). This simple rule-of-thumb suggests that the cyclic oligoacenes will be even more reactive than their linear counterparts, since it is not possible to form a Clar's sextet without unpaired electrons for the [n]CC family.

4.2.2 Geometrical and electronic features

To better understand the electronic structure of oligoacenes, we first explore their geometrical characteristics. The different contour conditions between the two families are reflected on the distribution of C-C bond lengths (Figure 2), with optimized geometries here in good agreement with previous DFT calculations.[84] In the cyclic molecules all edge and bridging bond distances are equal between themselves, the former being close to the typical distance in benzene (e.g. 1.41 Å for [11]CC) suggesting linear chain conjugation at the edges, an aspect with key implications that will be further analyzed in more detail along the study. The interchain bond (bridge) is much longer, e.g. 1.47 Å for [11]CC, corresponding to the bond distance of a single bond between two sp^2 C atoms. On the other hand, the linear acenes exhibit alternating edge distances with the two bonds at the molecular ends close to a double bond situation (Figure 2a). The bridging distances (Figure 2b) follow a continuous profile with shorter bonds at the ends and larger distances (closer to the cyclic case) at the center of the molecule.

View Article Online
DOI: 10.1039/C8CP00135A

This different structural topology between linear and cyclic acenes, namely the border vs. cyclic conditions, results in non-equivalence between central and edge C atoms in the linear family, and complete equivalence between all outer and inner (bridging) carbons for the cyclic acenes. This also has, in addition to the geometrical results described above, a strong impact on the electronic properties. In particular such differences results in qualitatively different molecular orbital diagrams, as recovered by the simple Hückel model as a proof of concept (Figure 3). The linear arrangement of benzene rings results in a set of non-degenerate orbitals around the Highest Occupied and Lowest Unoccupied Molecular Orbitals (HOMO and LUMO, respectively) with decreasing HOMO-LUMO gaps as the conjugation size of the system increases. On the other hand, the higher symmetry in the cyclic family results in sets of degenerate frontier orbitals. Moreover, the electronic distribution around the Fermi energy level is qualitatively different for molecules with an odd or even number of six-member rings. Cyclic acenes with an even number of rings present two electrons in two degenerate orbitals, predicting a strong diradical character, while [n]CC molecules with odd number of rings exhibit a pair of degenerate HOMOs and LUMOs with smaller energy gaps for larger systems. Hence, the Hückel model suggests that the electronic structure of cyclic oligoacenes hold sensible differences with respect to the linear counterparts, and that the odd and even members of the series follow rather different electronic structure patterns.

4.2.3 Evidences about the polyradical character

The spatial distribution of the unpaired electrons for linear oligoacenes represented by (FT-TPSS) FOD plots (Figure 4) and RAS-SF natural or-

View Article Online
DOI: 10.1039/C8CP00135A

bitals (Figure 5) suggests a growing polyradicaloid character with the number of fused rings, in qualitative agreement with the HOMO-LUMO gaps from the Hückel model, the symmetrized von Neumman entropy (see Figure S3) and the Hückel-based bond orders (see Figures S4-S5). Actually, Figure S6 also shows the exponential decay of N_{FOD} for linear oligoacenes as a function of the HOMO-LUMO energy difference. The unpaired density mostly lies on the non-bridging C atoms situated at both sides (up and down) of the molecule and mainly localizes on the central rings with virtually no contribution from the atoms at the molecular ends (left and right). This picture is obtained by both DFT (FT-TPSS) and wave function (RAS-SF) calculations, although the former produces larger delocalized FODs, which can be possibly associated with the lack of exact-exchange. The computed N_{FOD} values by both methods (FT-DFT results in Table S2 and RAS-SF results in Table S5) confirm the increasing diradicaloid nature (and SCE) along the linear oligoacene series, with values close to two unpaired electrons for the longest members of the series. The shortest oligoacenes (i.e. from naphthalene to tetracene) exhibit much weaker SCE, with $0.08 < N_{FOD} < 0.49$.

The unpaired electron density for the cyclic forms is delocalized along the entire nanoring and for the most part equally shared amongst the non-bridging C atoms (Figures 6 and 7). In general, the computed orbital occupancies and energies follow the scheme predicted by the Hückel model for the odd-numbered cyclic acenes, i.e. doubly degenerate HOMOs and LUMOs, while the frontier orbitals of $[n]$CC with $n = 6, 8, 10$ and 12 are no longer degenerate (as in Hückel) and present natural orbital occupancies and N_{FOD} values approximately corresponding to the case of two unpaired electrons (Tables S3 and S6), hence they can be labelled as diradicals (or

View Article Online
DOI: 10.1039/C8CP00135A

diradicaloids). On the other hand, [n]CC with $n = 5, 7, 9$ and 11 hold four natural orbitals with occupancies with sizable departure from the closed-shell configuration. These results suggest that odd cyclic oligoacenes contain four strongly correlated electrons and they should be treated as tetraradicaloid systems rather than diradicaloids.

Figure 8 shows the size-evolution of N_{FOD} along the two series, linear and cyclic acenes, obtained with the FT-TPSS method. The zig-zag profile drawn by the [n]CC family exposes the electronic differences between molecules with even and odd number of rings, with much larger values for odd n indicating close to four unpaired electrons in [11]CC. For linear oligoacenes there is a kind of cumulative effect, i.e. each C atoms contribute more and more to the radicaloid nature of the whole molecule and its number increases as the system grows. For cylic acenes, the increase in the N_{FOD} values with the number of rings is mostly due to an increase in the total number of unpaired electrons, as will be discussed in the next section, despite each C atom having a lower radicaloid character on average (see also Figures S3 and S5). Note finally that the highest value of N_{FOD} here obtained (4.259 for the [11]CC case) is significantly larger than any of the N_{FOD} values reported before for prototype systems displaying a truly multireference character, such as p-benzyne or the transition state of the Be–H_2 complex, as well as for studied biological systems such as the methylcobanimide cation.[63]

4.2.4 Interaction between radical rings

It is worth noting that in cyclic acenes with an even number of fused rings, the HONO (LUNO) presents "bonding" ("anti-bonding") interactions

View Article Online
DOI: 10.1039/C8CP00135A

between up and down edge (i.e. non-bridging) C atoms (Figure 7 (left)), while in linear and odd cyclic molecules the HONOs (LUNOs) correspond to the out-of-phase (in-phase) arrangement between up and down π-orbitals. This observation suggests that interaction between unpaired π-electrons at the edge carbons in even [n]CC lifts the degeneracy obtained with the Hückel model (Figure 3). Actually, if we add an additional (weak) interaction between each of these atom pairs in the Hückel Hamiltonian, we obtain a situation closer to the electronic structure calculations (Figure 9). The same interaction for odd n results in a decrease of the HOMO-LUMO gap.

To further explore the idea of interacting radical centers at the molecular edges we analyze the ground state RAS-SF wave functions of [n]CC with $n = 6, 8, 10$ and 12 by means of fragment decomposition.[85,86] In the fragment basis of up and down chains, the total wave function can be expressed in terms of covalent and ionic contributions as:

$$|\Psi\rangle = c_{cov}|\phi_u^{(1)}\phi_d^{(1)}\rangle + c_{ion}(|\phi_u^{(2)}\phi_d^{(0)}\rangle + |\phi_u^{(0)}\phi_d^{(2)}\rangle), \quad (6)$$

where ϕ_u and ϕ_d indicate up and down *radical rings*, the superindexes (m) indicate the number of electrons in each ring, and c_{cov} and c_{ion} are the coefficients for covalent and ionic contributions. The presence of ionic contributions is related to the ability of the two radical rings to share their electron density, thus it can be used as a measure of the strength of the inter-radical interaction. Stronger interaction between radical centers will result in larger orbital gaps and weaker diradical character. The correlation between ionic contributions and singlet-triplet gaps in Figure 10 rationalizes how the inter-radical ring interactions, equivalent to γ in the Hückel model, control and tune the strong diradical character in even cyclic acenes, with stronger interactions resulting in lower diradical character (larger HOMO-LUMO gaps).

View Article Online
DOI: 10.1039/C8CP00135A

4.2.5 The singlet-triplet energy gap

The diradical (or diradicaloid) character of ground state singlet wave functions has been systematically associated to small energy separation between the ground state singlet (S_0) and the lowest triplet state (T_1). Here we calculate the (vertical) singlet-triplet energy gap $\Delta E_{ST} = E(T_1) - E(S_0)$ in linear and cyclic oligoacenes by means of the FT-TPSS and RAS-SF models. Previous calculations for the longstanding quest of the ground-state nature of [n]CCs, and related isomers,[87,88] have shown the following: (i) a general failure of DFT calculations for predicting correctly the nature of their ground-state[89,90] unless for some last-generation orbital-optimized DFT-based methods[91] and/or double-hybrid functionals;[92] (ii) a significant multireference character of the prototype [6]CC molecule, with a ΔE_{ST} value of less than 0.04 eV at the MRMP2/6-31G*//CASSCF(8,8)/6-31G* level;[93] (iii) the existing difficulties for selecting systematically and routinely the (often large) CAS active spaces needed for the systematic study of [n]CCs of increasing size;[84,94] and (iv) the adequate alternative provided by TAO-DFT based methods[95] at a substantially lower computational cost.

Figure 11 displays the ΔE_{ST} results of the FT-TPSS calculations performed in this study, from which the odd-even pattern is also seen for [n]CC systems as well as the rapid decay for the linear systems in close agreement with RAS-SF and recent TAO-LDA results[95] (Table 1). It is worth noting the rather constant (and small) energy gap obtained for all the even cyclic acenes, which supports the idea of weak interactions between radical rings as the origin for singlet state stabilization. We also compare in Table 1 the

View Article Online
DOI: 10.1039/C8CP00135A

results obtained here with the best available, up to the best of our knowledge, multireference *ab initio* calculations,[84,94] to find a reasonable (semi-quantitative) agreement between this and the other approaches with some due caution with respect to the evolution with system size of the CASPT2 results. Overall, the cost-efficient FT-TPSS method exhibits very good results in the computation of singlet-triplet energy gaps at an impressively low computational effort.

4.2.6 Tetraradical character of odd cyclic acenes

As discussed above, the electronic structure analysis of the odd cyclic acenes suggests that they can be considered tetraradicaloids. The tetraradical character can be associated with small singlet-quintet energy difference, like singlet-triplet gaps relate to diradical character. Hence, we compute the energy gap to the lowest quintet state (Q_1) for [n]CC with $n = 5, 7, 9$ and 11 (see Table 2) to find that: (i) the vertical energy to Q_1 decrease with the molecular size, in good agreement with an increase of the tetraradical character with n; and (ii) the energy gaps to the lowest quintet are considerably low and similar to energy differences to T_1 for the largest cyclic acenes, i.e. $n = 9$ and 11.

4.3 Relating N_{FOD} to the bi- or polyradical character

The open-shell singlet biradical character of organic molecules has been recently related to the N_{FOD} values, thanks to the development of an experimental route in last years to gauge its character:[96]

$$y = 1 - \sqrt{1 - \left(\frac{E_{S_{1u},S_{1g}} - E_{T_{1u},S_{1g}}}{E_{S_{2g},S_{1g}}} \right)^2}, \qquad (7)$$

View Article Online
DOI: 10.1039/C8CP00135A

where all the excitation energies of the second right-hand side can be obtained from two-photon absorption, ESR, and phosphorescence experiments, and $0 \leq y \leq 1$ as limits for pure closed-shell or open-shell (biradical) nature.[97,98] According to the data reported before[64] for a set of some polycyclic aromatic molecules (including naphthalene, anthracene, fluorene, TIPS-pentacene, and chrysene) and a substituted hexaphyrin molecule, there is a linear relationship between y and the N_{FOD} values (see Figure S7 in the Supporting Information). Following that trend, we propose to distinguish between highly (slightly) pronounced polyradical ground-state character for organic molecules displaying $y \geq 0.5$ ($y < 0.5$) which is, in turn, roughly related to values of $N_{\mathrm{FOD}} \geq 1.5$ ($N_{\mathrm{FOD}} < 1.5$).

Following this approximate rule-of-thumb, we can label all [n]CC ([n]CPP) systems as having a pronounced (negligible) polyradical character, whereas for the case of linear oligoacenes there is a distinction between short (from naphthalene to hexacene) and long (from octacene to largest systems) molecules, with heptacene situated at the borderline ($N_{\mathrm{FOD}} \approx 1.5$) as also displayed in Figure 8. Actually, whereas systems as tetracene and pentacene are easy to functionalize and are being routinely exploited in many fields (e.g. Organic Electronics[99,100]), the situation becomes more involved for larger acenes. As a matter of example, heptacene has long been pursued and it was not until very recently that it could be isolated[12] and reported in bulk and at room-temperature.[13] Photogeneration of octacene and nonacene has made these systems accessible experimentally under the high-vacuum conditions required for matrix isolation,[101] with these and longer acenes constituting still a challenging synthetic effort.[102]

View Article Online
DOI: 10.1039/C8CP00135A

4.4 Molecular engineering of nanobelts

Herein we apply the FT-TPSS and RAS-SF approaches combined with the FOD analysis to the study of the electronic properties of other molecular nanobelts with distinct structural topologies, and we try to establish connections between their polyradicaloid character and structural motifs. First, we consider the distortion of the perfect loop in [n]CC to achieve the molecules named as cyclo[a]decacene and cyclo[a]undecacene, see their chemical structure in Figure 12. The rather small computed singlet-triplet energy gaps and considerable amount of unpaired electrons obtained by FOD analysis (Table 3) suggest important polyradical character pointing towards potential weak molecular stability that might limit their successful synthesis.

The different chemical topology at the kink breaks the perfect equivalence between benzene rings, which can be seen as the result of boundary conditions much like the molecular ends in linear acenes. Such contour conditions break the degeneracies between frontier orbitals (HOMOs and LUMOs) obtained in [n]CC molecules. As a result, cyclo[a]decacene and cyclo[a]undecacene present strong polyradical character with unpaired electrons localized mainly on the up and down (non-bridging) C atoms further from the kink. It is important to notice that their HONO and LUNO look like the ones obtained for linear acenes for both odd and even number of rings, that is a HONO and LUNO with out- and in-phase interaction between radical rings (Figure 13). These results clearly indicate that their electronic structure is closer to the linear acenes than to the [n]CC series.

Actually, we may conceive some other nanobelts with additional kinks, as those presented in Figure 12 too and dubbed as [3]cyclobenzo[a]anthracene

View Article Online
DOI: 10.1039/C8CP00135A

and [3]cyclochrysene. Note how the FOD plots, which needed to be done with a cut-off of $\sigma = 0.002$ e/bohr^3 to become visible, are delocalized but still absent from some C atoms. The N_{FOD} values are significantly lower than in any of the other studied nanobelts here, and closer to the [n]CPP series, indicating a rather weak diradicaloid character. Our results confirm the close relationships between SCE and structural motifs, hopefully paving also the way towards the molecular engineering of this kind of compounds.

5 Conclusions

We have studied a set of cyclic molecules of ongoing interest, named as [n]CPP or [n]CC, envisioned to act as molecular precursors for the fine-tuned synthesis of nanotubes of uniform diameter and controlled edges. The accurate modelling of these molecules might need the use of methods incorporating strong correlation effects, and we have thus systematically employed the tool known as FOD and the RAS-SF method to reveal this nature. While the former tool provides not only a real-space representation of these electron-correlation effects, but some global indicators (e.g. the integrated number of electrons arising from the fractional occupation of orbitals, N_{FOD}) allowing to distinguish and then classify the molecules as bi- or poly-radicals, the latter provides a multi-configurational wave function description able to accommodate and describe to a great detail a several strongly correlated electrons.

Our calculations suggest a strong relationship between polyradical character and the structural motifs forming the nanoring, with a particular distinction between cyclic phenylenes or cyclic acenes. The latter are known to be a longstanding synthetic target not still achieved, closely related with

View Article Online
DOI: 10.1039/C8CP00135A

the longest parent linear compounds as the calculations unveiled. Detailed analysis of the ground and low-lying states of these molecules suggests that odd and even [n]CC oligomers should be treated as separate families with diradical and tetraradical character, respectively. They exhibit qualitative differences in their electronic structure around the frontier orbitals, resulting in a small and rather constant singlet-triplet energy gaps for the even series and with small and decreasing singlet-quintet gaps for the odd cyclacenes. We have also tried to relate the cyclic molecular shape and the envisioned synthesis of nanobelts, starting from the [n]CC forms, with some kinks or defects being prone to break the strong correlation effects found in pristine [n]CC compounds.

Acknowledgements

A.J.P.J. and J.C.S.G acknowledge the "Ministerio de Economía y Competitividad" of Spain and the "European Regional Development Fund" through the project CTQ2014-55073-P, and E.S.F.M. through the project FIS2015-64222-C2-2-P. D.C. is thankful to Eusko Jaurlaritza and the Spanish Government MINECO/FEDER (projects IT588-13 and CTQ2016-80955). M.E.S.-S. acknowledges CONACyT-México for a Ph.D. fellowship (ref. 591700).

Associated content

The Supporting Information contains in this order: (i) Figure S1 with the correlation between N_{FOD} values obtained by FT-DFT and RAS-SF methods; (ii) Figure S2 illustrating the resonance structures found for linear and cyclic acenes, with Clar's sextet ring indicated in blue; (iii) a discussion about the symmetrized von Neumann entropy, and its evolution (Figure S3)

View Article Online
DOI: 10.1039/C8CP00135A

as a function of the number of C atoms for linear and cyclic oligoacenes; (iv) Figures S4-S5 showing the evolution of the radicaloid character for linear and cyclic oligoacenes, as deduced from bond orders obtained at the Hückel level; (v) Figure S6 displaying the relationship between N_{FOD} and the HOMO-LUMO energy difference for linear oligoacenes; (vi) Figure S7 with the relationship between y (biradical character) and N_{FOD} values; (vii) Tables S1-S4 with the energies and fractional occupation numbers of the (H-4)OMO to (L+4)UMO window of orbitals for each of the [n]CPP, linear and cyclic compounds, and the other engineered nanobelts; (viii) Tables S5-S6 with the natural occupation numbers of the (H-3)OMO to the (L+3)UNO window of orbitals for each of the linear and cyclic compounds; and (ix) Table S7 with the optimized Cartesian coordinates of all relevant compounds.

Author contributions

A.P.G. and M.E.S.S. contributed equally to this work. The manuscript was written through contributions of all authors. All authors have given approval to the final version of the manuscript.

References

[1] Omachi, H.; Segawa, Y.; Itami, K. Synthesis of Cycloparaphenylenes and Related Carbon Nanorings: A Step Toward the Controlled Synthesis of Carbon Nanotubes. *Accounts of Chemical Research* **2012**, *45*, 1378–1389.

[2] Segawa, Y.; Fukazawa, A.; Matsuura, S.; Omachi, H.; Yamaguchi, S.; Irle, S.; Itami, K. Combined Experimental and Theoretical Studies

View Article Online
DOI: 10.1039/C8CP00135A

on the Photophysical Properties of Cycloparaphenylenes. *Organic & Biomolecular Chemistry* **2012**, *10*, 5979–5984.

[3] Hirst, E. S.; Jasti, R. Bending Benzene: Syntheses of [n]Cycloparaphenylenes. *The Journal of Organic Chemistry* **2012**, *77*, 10473–10478.

[4] Yamago, S.; Kayahara, E.; Iwamoto, T. Organoplatinum-Mediated Synthesis of Cyclic π-Conjugated Molecules: Towards a New Era of Three-Dimensional Aromatic Compounds. *The Chemical Record* **2014**, *14*, 84–100.

[5] Golder, M. R.; Jasti, R. Syntheses of the Smallest Carbon Nanohoops and the Emergence of Unique Physical Phenomena. *Accounts of Chemical Research* **2015**, *48*, 557–566.

[6] Kayahara, E.; Patel, V. K.; Xia, J.; Jasti, R.; Yamago, S. Selective and Gram-Scale Synthesis of [6]Cycloparaphenylene. *Synlett* **2015**, *26*, 1615–1619.

[7] Darzi, E. R.; Jasti, R. The Dynamic, Size-Dependent Properties of [5]-[12]Cycloparaphenylenes. *Chemical Society Reviews* **2015**, *44*, 6401–6410.

[8] Segawa, Y.; Yagi, A.; Matsui, K.; Itami, K. Design and Synthesis of Carbon Nanotube Segments. *Angewandte Chemie International Edition* **2016**, *55*, 5136–5158.

[9] Omachi, H.; Nakayama, T.; Takahashi, E.; Segawa, Y.; Itami, K. Initiation of Carbon Nanotube Growth by Well-defined Carbon Nanorings. *Nature Chemistry* **2013**, *5*, 572–576.

View Article Online
DOI: 10.1039/C8CP00135A

[10] Lu, X.; Wu, J. After 60 Years of Efforts: The Chemical Synthesis of a Carbon Nanobelt. *Chem* **2017**, *2*, 619–620.

[11] Watanabe, M.; Chang, Y. J.; Liu, S.-W.; Chao, T.-H.; Goto, K.; Islam, M. M.; Yuan, C.-H.; Tao, Y.-T.; Shinmyozu, T.; Chow, T. J. The Synthesis, Crystal Structure and Charge-Transport Properties of Hexacene. *Nature Chemistry* **2012**, *4*, 574–578.

[12] Mondal, R.; Shah, B. K.; Neckers, D. C. Photogeneration of Heptacene in a Polymer Matrix. *Journal of the American Chemical Society* **2006**, *128*, 9612–9613.

[13] Einholz, R.; Fang, T.; Berger, R.; Gruninger, P.; Fruh, A.; Chasse, T.; Fink, R. F.; Bettinger, H. F. Heptacene: Characterization in Solution, in the Solid State, and in Films. *Journal of the American Chemical Society* **2017**, *139*, 4435–4442.

[14] Purushothaman, B.; Bruzek, M.; Parkin, S. R.; Miller, A.-F.; Anthony, J. E. Synthesis and Structural Characterization of Crystalline Nonacenes. *Angewandte Chemie* **2011**, *123*, 7151–7155.

[15] Povie, G.; Segawa, Y.; Nishihara, T.; Miyauchi, Y.; Itami, K. Synthesis of a Carbon Nanobelt. *Science* **2017**, *356*, 172–175.

[16] Handy, N. C.; Cohen, A. J. Left-right Correlation Energy. *Molecular Physics* **2001**, *99*, 403–412.

[17] Tew, D. P.; Klopper, W.; Helgaker, T. Electron Correlation: The Many-Body Problem at the Heart of Chemistry. *Journal of Computational Chemistry* **2007**, *28*, 1307–1320.

View Article Online
DOI: 10.1039/C8CP00135A

[18] Cohen, A. J.; Mori-Sánchez, P.; Yang, W. Insights Into Current Limitations of Density Functional Theory. *Science* **2008**, *321*, 792–794.

[19] Cohen, A. J.; Mori-Sánchez, P.; Yang, W. Challenges for Density Functional Theory. *Chemical Reviews* **2011**, *112*, 289–320.

[20] Lee, J.; Small, D. W.; Epifanovsky, E.; Head-Gordon, M. Coupled-Cluster Valence-Bond Singles and Doubles for Strongly Correlated Systems: Block-tensor Based Implementation and Application to Oligoacenes. *Journal of Chemical Theory and Computation* **2017**, *13*, 602–615.

[21] Pérez-Jiménez, Á. J.; Pérez-Jordá, J. M. Combining Multiconfigurational Wave Functions With Correlation Density Functionals: A Size-Consistent Method Based on Natural Orbitals and Occupation Numbers. *Physical Review A* **2007**, *75*, 012503.

[22] Matito, E.; Casanova, D.; Lopez, X.; Ugalde, J. M. Exact Exchange–Correlation Functional for the Infinitely Stretched Hydrogen Molecule. *Theoretical Chemistry Accounts* **2016**, *135*, 226.

[23] Rodríguez-Mayorga, M.; Ramos-Cordoba, E.; Via-Nadal, M.; Piris, M.; Matito, E. Comprehensive Benchmarking of Density Matrix Functional Approximations. *Physical Chemistry Chemical Physics* **2017**, *19*, 24029–24041.

[24] Ryabinkin, I. G.; Ospadov, E.; Staroverov, V. N. Exact Exchange-Correlation Potentials of Singlet Two-Electron Systems. *The Journal of Chemical Physics* **2017**, *147*, 164117.

[25] Lee, T. J.; Taylor, P. R. A Diagnostic for Determining the Quality of

View Article Online
DOI: 10.1039/C8CP00135A

Single-Reference Electron Correlation Methods. *International Journal of Quantum Chemistry* **1989**, *36*, 199–207.

[26] Lee, T. J. Comparison of the T_1 and D_1 Diagnostics for Electronic Structure Theory: A New Definition for the Open-Shell D_1 Diagnostic. *Chemical Physics Letters* **2003**, *372*, 362–367.

[27] Fogueri, U. R.; Kozuch, S.; Karton, A.; Martin, J. M. A Simple DFT-based Diagnostic for Nondynamical Correlation. *Theoretical Chemistry Accounts* **2013**, *132*, 1291.

[28] Ramos-Cordoba, E.; Matito, E. Local Descriptors of Dynamic and Non-dynamic Correlation. *Journal of Chemical Theory and Computation* **2017**, *13*, 2705–2711.

[29] Moscardó, F.; San-Fabián, E. Density-Functional Formalism and the Two-Body Problem. *Physical Review A* **1991**, *44*, 1549.

[30] Perdew, J. P.; Savin, A.; Burke, K. Escaping the Symmetry Dilemma through a Pair-Density Interpretation of Spin-Density Functional Theory. *Physical Review A* **1995**, *51*, 4531.

[31] Miehlich, B. B.; Stoll, H.; Savin, A. A Correlation-Energy Density Functional for Multideterminantal Wavefunctions. *Molecular Physics* **1997**, *91*, 527–536.

[32] Moscardó, F.; Pérez-Jiménez, A. J. Self-Consistent Field Calculations Using Two-Body Density Functionals for Correlation Energy Component: I. Atomic Systems. *Journal of Computational Chemistry* **1998**, *19*, 1887–1898.

View Article Online
DOI: 10.1039/C8CP00135A

[33] Moscardó, F.; Pérez-Jiménez, A. J.; Cjuno, J. A. Self-Consistent Field Calculations Using Two-Body Density Functionals for Correlation Energy Component: II. Small Molecules. *Journal of Computational Chemistry* **1998**, *19*, 1899–1908.

[34] McDouall, J. J. Combining Two-Body Density Functionals with Multiconfigurational Wavefunctions: Diatomic Molecules. *Molecular Physics* **2003**, *101*, 361–371.

[35] Sancho-García, J. C.; Moscardó, F. Usefulness of the Colle–Salvetti Model for the Treatment of the Nondynamic Correlation. *The Journal of Chemical Physics* **2003**, *118*, 1054–1058.

[36] Takeda, R.; Yamanaka, S.; Yamaguchi, K. Approximate On-Top Pair Density into One-Body Functions for CAS-DFT. *International Journal of Quantum Chemistry* **2004**, *96*, 463–473.

[37] Gusarov, S.; Malmqvist, P.-Å.; Lindh, R. Using On-Top Pair Density for Construction of Correlation Functionals for Multideterminant Wave Functions. *Molecular Physics* **2004**, *102*, 2207–2216.

[38] Toulouse, J.; Colonna, F.; Savin, A. Long-Range–Short-Range Separation of the Electron-Electron Interaction in Density-Functional Theory. *Physical Review A* **2004**, *70*, 062505.

[39] Filatov, M.; Shaik, S. A Spin-Restricted Ensemble-Referenced Kohn–Sham Method and its Application to Diradicaloid Situations. *Chemical Physics Letters* **1999**, *304*, 429–437.

[40] Kazaryan, A.; Heuver, J.; Filatov, M. Excitation Energies from Spin-Restricted Ensemble-Referenced Kohn–Sham Method: A State-

View Article Online
DOI: 10.1039/C8CP00135A

Average Approach. *The Journal of Physical Chemistry A* **2008**, *112*, 12980–12988.

[41] Filatov, M. Spin-Restricted Ensemble-Referenced Kohn–Sham Method: Basic Principles and Application to Strongly Correlated Ground and Excited States of Molecules. *Wiley Interdisciplinary Reviews: Computational Molecular Science* **2015**, *5*, 146–167.

[42] Grimme, S.; Waletzke, M. A Combination of Kohn–Sham Density Functional Theory and Multi-Reference Configuration Interaction Methods. *The Journal of Chemical Physics* **1999**, *111*, 5645–5655.

[43] Gräfenstein, J.; Cremer, D. The Combination of Density Functional Theory with Multi-Configuration Methods–CAS-DFT. *Chemical Physics Letters* **2000**, *316*, 569–577.

[44] Nakata, K.; Ukai, T.; Yamanaka, S.; Takada, T.; Yamaguchi, K. CASSCF Version of Density Functional Theory. *International Journal of Quantum Chemistry* **2006**, *106*, 3325–3333.

[45] Pijeau, S.; Hohenstein, E. G. Improved Complete Active Space Configuration Interaction Energies with a Simple Correction from Density Functional Theory. *Journal of Chemical Theory and Computation* **2017**, *13*, 1130–1146.

[46] Garza, A. J.; Jiménez-Hoyos, C. A.; Scuseria, G. E. Capturing Static and Dynamic Correlations by a Combination of Projected Hartree–Fock and Density Functional Theories. *The Journal of Chemical Physics* **2013**, *138*, 134102.

[47] Rivero, P.; Jiménez-Hoyos, C. A.; Scuseria, G. E. Entanglement and Polyradical Character of Polycyclic Aromatic Hydrocarbons Predicted

View Article Online
DOI: 10.1039/C8CP00135A

by Projected Hartree–Fock Theory. *The Journal of Physical Chemistry B* **2013**, *117*, 12750–12758.

[48] Shao, Y.; Head-Gordon, M.; Krylov, A. I. The Spin–Flip Approach within Time-Dependent Density Functional Theory: Theory and Applications to Diradicals. *The Journal of Chemical Physics* **2003**, *118*, 4807–4818.

[49] Becke, A. D. Real-Space Post-Hartree–Fock Correlation Models. *The Journal of Chemical Physics* **2005**, *122*, 064101.

[50] Pérez-Jiménez, Á. J.; Pérez-Jordá, J. M.; Sancho-García, J. C. Combining Two-Body Density Correlation Functionals with Multiconfigurational Wave Functions Using Natural Orbitals and Occupation Numbers. *The Journal of Chemical Physics* **2007**, *127*, 104102.

[51] Piris, M.; Lopez, X.; Ruipérez, F.; Matxain, J.; Ugalde, J. A Natural Orbital Functional for Multiconfigurational States. *The Journal of Chemical Physics* **2011**, *134*, 164102.

[52] Piris, M.; Ugalde, J. M. Perspective on Natural Orbital Functional Theory. *International Journal of Quantum Chemistry* **2014**, *114*, 1169–1175.

[53] Ess, D. H.; Johnson, E. R.; Hu, X.; Yang, W. Singlet- Triplet Energy Gaps for Diradicals from Fractional-Spin Density-Functional Theory. *The Journal of Physical Chemistry A* **2010**, *115*, 76–83.

[54] Li Manni, G.; Carlson, R. K.; Luo, S.; Ma, D.; Olsen, J.; Truhlar, D. G.; Gagliardi, L. Multiconfiguration Pair-Density Functional Theory. *Journal of Chemical Theory and Computation* **2014**, *10*, 3669–3680.

View Article Online
DOI: 10.1039/C8CP00135A

[55] Gagliardi, L.; Truhlar, D. G.; Li Manni, G.; Carlson, R. K.; Hoyer, C. E.; Bao, J. L. Multiconfiguration Pair-Density Functional Theory: A New Way to Treat Strongly Correlated Systems. *Accounts of Chemical Research* **2016**, *50*, 66–73.

[56] Hoyer, C. E.; Ghosh, S.; Truhlar, D. G.; Gagliardi, L. Multiconfiguration Pair-Density Functional Theory is as Accurate as CASPT2 for Electronic Excitation. *The Journal of Physical Chemistry Letters* **2016**, *7*, 586–591.

[57] Ghosh, S.; Cramer, C. J.; Truhlar, D. G.; Gagliardi, L. Generalized-Active-Space Pair-Density Functional Theory: An Efficient Method to Study Large, Strongly Correlated, Conjugated Systems. *Chemical Science* **2017**, *8*, 2741–2750.

[58] Grimme, S. Towards First Principles Calculation of Electron Impact Mass Spectra of Molecules. *Angewandte Chemie International Edition* **2013**, *52*, 6306–6312.

[59] Chai, J.-D. Thermally-Assisted-Occupation Density Functional Theory with Generalized-Gradient Approximations. *The Journal of Chemical Physics* **2014**, *140*, 18A521.

[60] Lin, C.-Y.; Hui, K.; Chung, J.-H.; Chai, J.-D. Self-Consistent Determination of the Fictitious Temperature in Thermally-Assisted-Occupation Density Functional Theory. *RSC Advances* **2017**, *7*, 50496–50507.

[61] Mermin, N. D. Thermal Properties of the Inhomogeneous Electron Gas. *Physical Review* **1965**, *137*, A1441.

View Article Online
DOI: 10.1039/C8CP00135A

[62] Chai, J.-D. Density Functional Theory with Fractional Orbital Occupations. *The Journal of Chemical Physics* **2012**, *136*, 154104.

[63] Grimme, S.; Hansen, A. A Practicable Real-Space Measure and Visualization of Static Electron-Correlation Effects. *Angewandte Chemie International Edition* **2015**, *54*, 12308–12313.

[64] Bauer, C. A.; Hansen, A.; Grimme, S. The Fractional Occupation Number Weighted Density as a Versatile Analysis Tool for Molecules with a Complicated Electronic Structure. *Chemistry-A European Journal* **2017**, *23*, 6150–6164.

[65] Casanova, D.; Head-Gordon, M. Restricted Active Space Spin-Flip Configuration Interaction Approach: Theory, Implementation and Examples. *Physical Chemistry Chemical Physics* **2009**, *11*, 9779–9790.

[66] Plasser, F.; Pašalić, H.; Gerzabek, M. H.; Libisch, F.; Reiter, R.; Burgdörfer, J.; Müller, T.; Shepard, R.; Lischka, H. The Multiradical Character of One-and Two-Dimensional Graphene Nanoribbons. *Angewandte Chemie International Edition* **2013**, *52*, 2581–2584.

[67] Horn, S.; Plasser, F.; Müller, T.; Libisch, F.; Burgdörfer, J.; Lischka, H. A Comparison of Singlet and Triplet States for One-and Two-dimensional Graphene Nanoribbons Using Multireference Theory. *Theoretical Chemistry Accounts* **2014**, *133*, 1511.

[68] Das, A.; Muller, T.; Plasser, F.; Lischka, H. Polyradical Character of Triangular Non-Kekulé Structures, Zethrenes, p-Quinodimethane-Linked Bisphenalenyl, and the Clar Goblet in Comparison: An Extended Multireference Study. *The Journal of Physical Chemistry A* **2016**, *120*, 1625–1636.

View Article Online
DOI: 10.1039/C8CP00135A

[69] Krylov, A. I. Spin-Flip Configuration Interaction: An Electronic Structure Model that is both Variational and Size-Consistent. *Chemical Physics Letters* **2001**, *350*, 522–530.

[70] Krylov, A. I. Spin-flip Equation-of-Motion Coupled-Cluster Electronic Structure Method for a Description of Excited States, Bond Breaking, Diradicals, and Triradicals. *Accounts of Chemical Research* **2006**, *39*, 83–91.

[71] Head-Gordon, M. Characterizing Unpaired Electrons from the One-Particle Density Matrix. *Chemical Physics Letters* **2003**, *372*, 508–511.

[72] Frisch, M. J. et al. Gaussian 09 Revision E.01. Gaussian Inc. Wallingford CT 2009.

[73] Zhao, Y.; Truhlar, D. G. The M06 Suite of Density Functionals for Main Group Thermochemistry, Thermochemical Kinetics, Noncovalent Interactions, Excited States, and Transition Elements: Two New Functionals and Systematic Testing of Four M06-class Functionals and 12 Other Functionals. *Theoretical Chemistry Accounts* **2008**, *120*, 215–241.

[74] San-Fabián, E.; Pérez-Guardiola, A.; Moral, M.; Pérez-Jiménez, A. J.; Sancho-García, J. C. Theoretical Study of Strained Carbon-based Nanobelts: Structural, Energetic, Electronic, and Magnetic Properties of [n] Cyclacenes. *Advanced Magnetic and Optical Materials* **2016**, 165–183.

[75] Neese, F. The ORCA Program System. *Wiley Interdisciplinary Reviews: Computational Molecular Science* **2012**, *2*, 73–78.

View Article Online
DOI: 10.1039/C8CP00135A

[76] Pettersen, E. F.; Goddard, T. D.; Huang, C. C.; Couch, G. S.; Greenblatt, D. M.; Meng, E. C.; Ferrin, T. E. UCSF Chimera: A Visualization System for Exploratory Research and Analysis. *Journal of Computational Chemistry* **2004**, *25*, 1605–1612.

[77] Shao et al., Y. Advances in Molecular Quantum Chemistry Contained in the Q-Chem 4 Program Package. *Molecular Physics* **2015**, *113*, 184–215.

[78] Xia, J.; Bacon, J. W.; Jasti, R. Gram-Scale Synthesis and Crystal Structures of [8] and [10]CPP, and the Solid-State Structure of C_{60}-[10]CPP. *Chemical Science* **2012**, *3*, 3018–3021.

[79] Reche-Tamayo, M.; Moral, M.; Pérez-Jiménez, A. J.; Sancho-García, J. C. Theoretical Determination of Interaction and Cohesive Energies of Weakly Bound Cycloparaphenylene Molecules. *The Journal of Physical Chemistry C* **2016**, *120*, 22627–22634.

[80] Iwamoto, T.; Watanabe, Y.; Sadahiro, T.; Haino, T.; Yamago, S. Size-Selective Encapsulation of C_{60} by [10]Cycloparaphenylene: Formation of the Shortest Fullerene-Peapod. *Angewandte Chemie International Edition* **2011**, *50*, 8342–8344.

[81] Iwamoto, T.; Watanabe, Y.; Takaya, H.; Haino, T.; Yasuda, N.; Yamago, S. Size-and Orientation-Selective Encapsulation of C_{70} by Cycloparaphenylenes. *Chemistry–A European Journal* **2013**, *19*, 14061–14068.

[82] Iwamoto, T.; Slanina, Z.; Mizorogi, N.; Guo, J.; Akasaka, T.; Nagase, S.; Takaya, H.; Yasuda, N.; Kato, T.; Yamago, S. Partial Charge

View Article Online
DOI: 10.1039/C8CP00135A

Transfer in the Shortest Possible Metallofullerene Peapod, LaC_{82}-[11]Cycloparaphenylene. *Chemistry–A European Journal* **2014**, *20*, 14403–14409.

[83] Xia, J.; Golder, M. R.; Foster, M. E.; Wong, B. M.; Jasti, R. Synthesis, Characterization, and Computational Studies of Cycloparaphenylene Dimers. *Journal of the American Chemical Society* **2012**, *134*, 19709–19715.

[84] Sadowsky, D.; McNeill, K.; Cramer, C. J. Electronic Structures of [n]-Cyclacenes ($n = 6 - 12$) and Short, Hydrogen-Capped, Carbon Nanotubes. *Faraday Discussions* **2010**, *145*, 507–521.

[85] Luzanov, A. V.; Casanova, D.; Feng, X.; Krylov, A. I. Quantifying Charge Resonance and Multiexciton Character in Coupled Chromophores by Charge and Spin Cumulant Analysis. *The Journal of Chemical Physics* **2015**, *142*, 224104.

[86] Casanova, D.; Krylov, A. I. Quantifying Local Exciton, Charge Resonance, and Multiexciton Character in Correlated Wave Functions of Multichromophoric Systems. *The Journal of Chemical Physics* **2016**, *144*, 014102.

[87] Hirst, E. S.; Wang, F.; Jasti, R. Theoretical Analysis of $[5.7]_n$Cyclacenes: Closed-Shell Cyclacene Isomers. *Organic letters* **2011**, *13*, 6220–6223.

[88] Esser, B. Theoretical Analysis of [5.5.6]Cyclacenes: Electronic Properties, Strain Energies and Substituent Effects. *Physical Chemistry Chemical Physics* **2015**, *17*, 7366–7372.

View Article Online
DOI: 10.1039/C8CP00135A

[89] Choi, H. S.; Kim, K. S. Structures, Magnetic Properties, and Aromaticity of Cyclacenes. *Angewandte Chemie International Edition* **1999**, *38*, 2256–2258.

[90] Houk, K.; Lee, P. S.; Nendel, M. Polyacene and Cyclacene Geometries and Electronic Structures: Bond Equalization, Vanishing Band Gaps, and Triplet Ground States Contrast with Polyacetylene. *The Journal of Organic Chemistry* **2001**, *66*, 5517–5521.

[91] Sancho-García, J.-C.; Pérez-Jiménez, A. J.; Savarese, M.; Brémond, E.; Adamo, C. Importance of Orbital Optimization for Double-Hybrid Density Functionals: Application of the OO-PBE-QIDH Model for Closed-and Open-Shell Systems. *The Journal of Physical Chemistry A* **2016**, *120*, 1756–1762.

[92] Grimme, S.; Steinmetz, M. A Computationally Efficient Double Hybrid Density Functional Based on the Random Phase Approximation. *Physical Chemistry Chemical Physics* **2016**, *18*, 20926–20937.

[93] Chen, Z.; Jiang, D.-e.; Lu, X.; Bettinger, H. F.; Dai, S.; Schleyer, P. v. R.; Houk, K. N. Open-Shell Singlet Character of Cyclacenes and Short Zigzag Nanotubes. *Organic Letters* **2007**, *9*, 5449–5452.

[94] Battaglia, S.; Faginas-Lago, N.; Andrae, D.; Evangelisti, S.; Leininger, T. Increasing Radical Character of Large [*n*]Cyclacenes Unveiled by Wave Function Theory. *The Journal of Physical Chemistry A* **2017**, *121*, 3746–3756.

[95] Wu, C.; Lee, P.; Chai, J. Electronic Properties of Cyclacenes from TAO-DFT. *Scientific Reports* **2016**, *6*, 37249.

View Article Online
DOI: 10.1039/C8CP00135A

[96] Nakano, M.; Kishi, R.; Ohta, S.; Takahashi, H.; Kubo, T.; Kamada, K.; Ohta, K.; Botek, E.; Champagne, B. Relationship Between Third-Order Nonlinear Optical Properties and Magnetic Interactions in Open-Shell Systems: A New Paradigm for Nonlinear Optics. *Physical Review Letters* **2007**, *99*, 033001.

[97] Kamada, K.; Ohta, K.; Kubo, T.; Shimizu, A.; Morita, Y.; Nakasuji, K.; Kishi, R.; Ohta, S.; Furukawa, S.-i.; Takahashi, H.; Nakano, M. Strong Two-Photon Absorption of Singlet Diradical Hydrocarbons. *Angewandte Chemie* **2007**, *119*, 3614–3616.

[98] Kamada, K.; Ohta, K.; Shimizu, A.; Kubo, T.; Kishi, R.; Takahashi, H.; Botek, E.; Champagne, B.; Nakano, M. Singlet Diradical Character from Experiment. *The Journal of Physical Chemistry Letters* **2010**, *1*, 937–940.

[99] Anthony, J. E. The Larger Acenes: Versatile Organic Semiconductors. *Angewandte Chemie International Edition* **2008**, *47*, 452–483.

[100] Casanova, D. Electronic Structure Study of Singlet Fission in Tetracene Derivatives. *Journal of Chemical Theory and Computation* **2013**, *10*, 324–334.

[101] Tönshoff, C.; Bettinger, H. F. Photogeneration of Octacene and Nonacene. *Angewandte Chemie International Edition* **2010**, *49*, 4125–4128.

[102] Huang, R.; Phan, H.; Herng, T. S.; Hu, P.; Zeng, W.; Dong, S.-q.; Das, S.; Shen, Y.; Ding, J.; Casanova, D.; Wu, J. Higher Order π-Conjugated Polycyclic Hydrocarbons with Open-Shell Singlet Ground

View Article Online
DOI: 10.1039/C8CP00135A

State: Nonazethrene versus Nonacene. *Journal of the American Chemical Society* **2016**, *138*, 10323–10330.

View Article Online
DOI: 10.1039/C8CP00135A

Table 1: Comparison between calculated ΔE_{ST} values (in eV) for $[n]$CCs of increasing size ($n = 5 - 12$).

System	RAS-SF	FT-TPSS	CASPT2/6-31G*[a]	NEVPT2/ANO-DZP[b]	TAO-LDA[c]
$n = 5$	0.854	0.302	–	–	0.26
$n = 6$	0.264	0.419	0.52	0.36	0.43
$n = 7$	0.356	0.294	0.52	–	0.26
$n = 8$	0.255	0.404	0.63	0.41	0.48
$n = 9$	0.164	0.255	0.35	–	0.12
$n = 10$	0.258	0.304	0.49	0.44	0.39
$n = 11$	0.112	0.232	0.32	–	0.11
$n = 12$	0.228	0.231	0.60	0.33	0.28

[a] Values taken from Ref.[84]
[b] Values taken from Ref.[94]
[c] Values taken from Ref.[95]

View Article Online
DOI: 10.1039/C8CP00135A

Table 2: RAS-SF calculated energy gaps (eV) to the second triplet (T_2) and lowest quintet states (Q_1) for odd $[n]$CCs.

System	ΔE_{ST_2}	ΔE_{SQ_1}
$n = 5$	1.147	2.068
$n = 7$	0.812	0.842
$n = 9$	0.568	0.399
$n = 11$	0.421	0.284

View Article Online
DOI: 10.1039/C8CP00135A

Table 3: Comparison between RAS-SF and FT-TPSS calculated ΔE_{ST} values (in eV) and N_{FOD} for cyclo[a]decacene and cyclo[a]undecacene molecules.

	RAS-SF		FT-TPSS	
System	ΔE_{ST}	N_{FOD}	ΔE_{ST}	N_{FOD}
cyclo[a]decacene	0.138	1.82	0.354	2.59
cyclo[a]undecacene	0.151	1.99	0.304	2.88

View Article Online
DOI: 10.1039/C8CP00135A

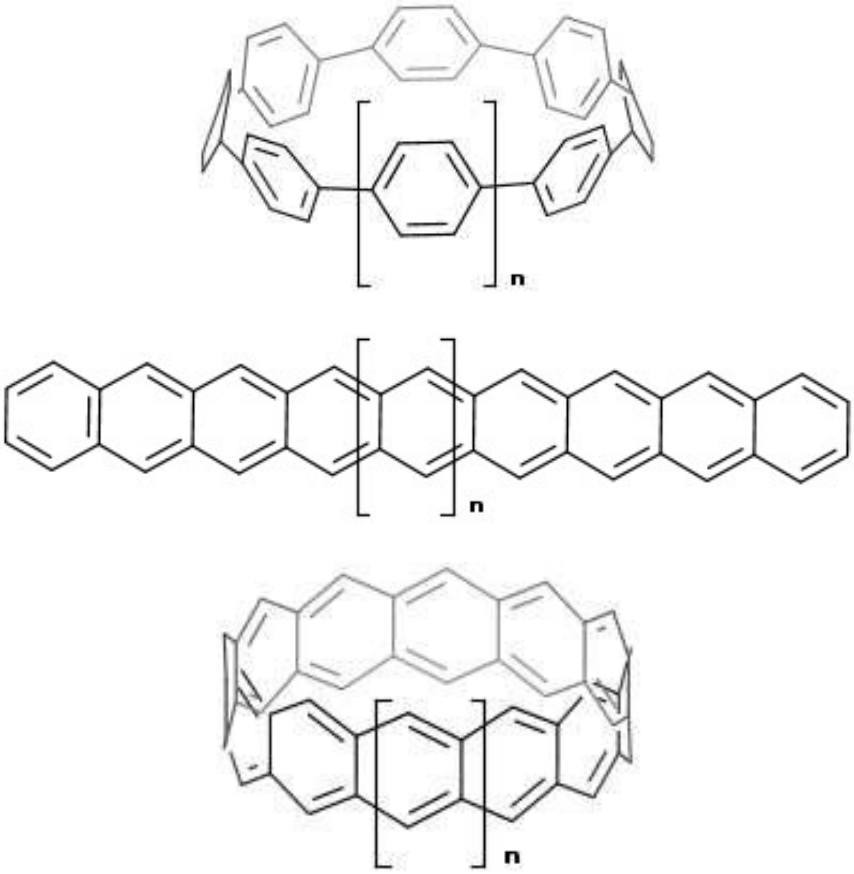

Figure 1: Chemical structures (from top to bottom) of $[n]$CPP, linear oligoacene, and $[n]$CC systems, with H atoms omitted for clarity.

View Article Online
DOI: 10.1039/C8CP00135A

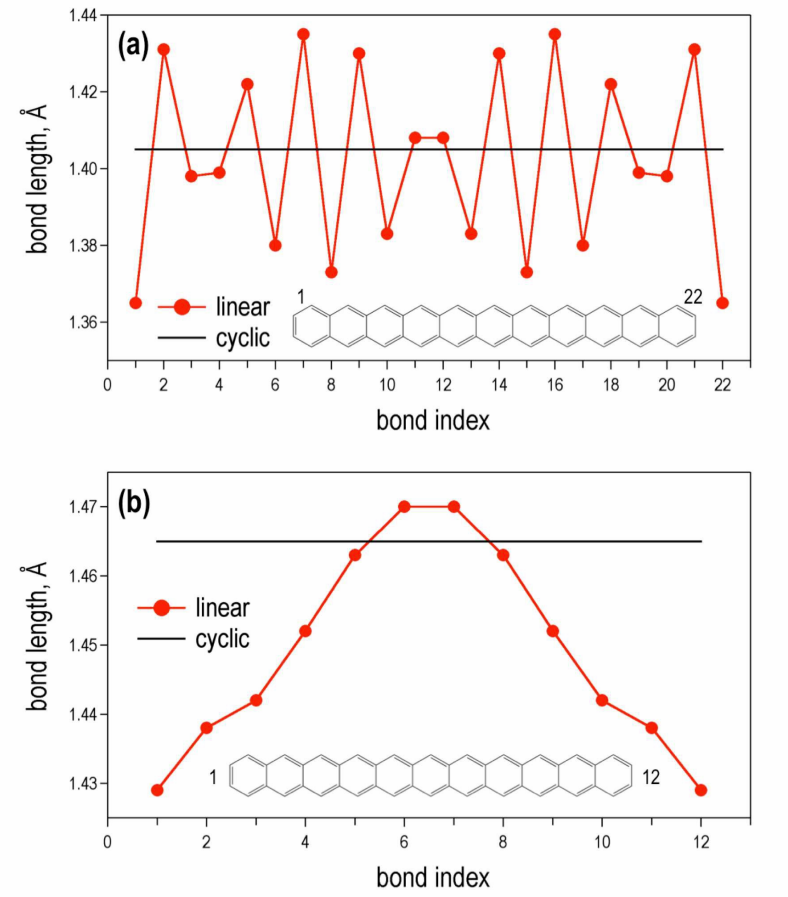

Figure 2: Consecutive C-C edge (top) and bridge (bottom) bond lengths for the linear (undecacene, red) and cyclic ([11]CC, black) oligoacenes.

View Article Online
DOI: 10.1039/C8CP00135A

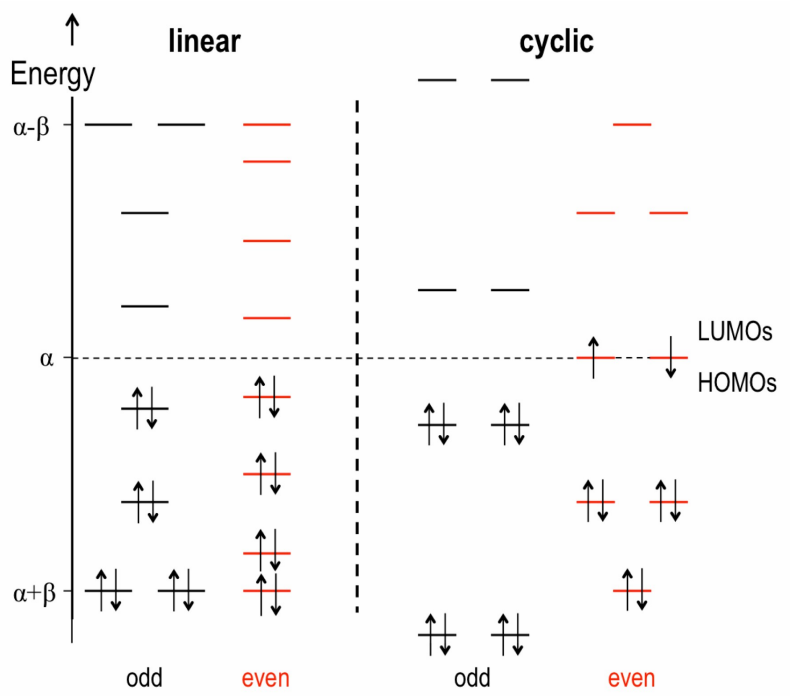

Figure 3: Hückel molecular orbital energy diagram around the Fermi energy level ($E = \alpha$) for linear (left) and cyclic (right) acenes with an odd ($n = 5$) and even ($n = 6$) fused rings.

View Article Online
DOI: 10.1039/C8CP00135A

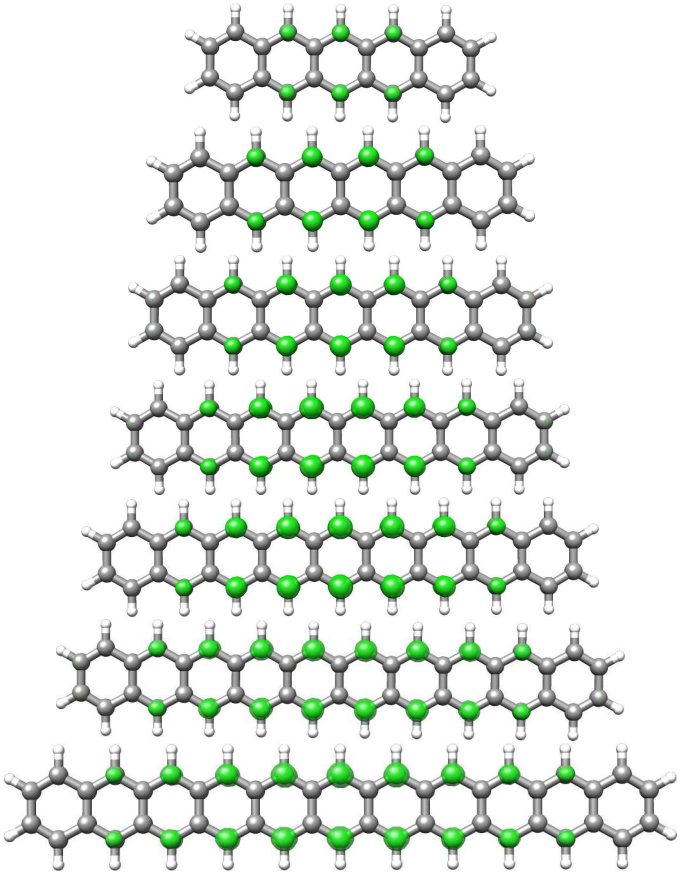

Figure 4: Plots of the FOD density (σ = 0.005 e/bohr^3) for oligoacenes ranging from pentacene (top) to undecacene (bottom), as obtained from the FT-DFT method.

View Article Online
DOI: 10.1039/C8CP00135A

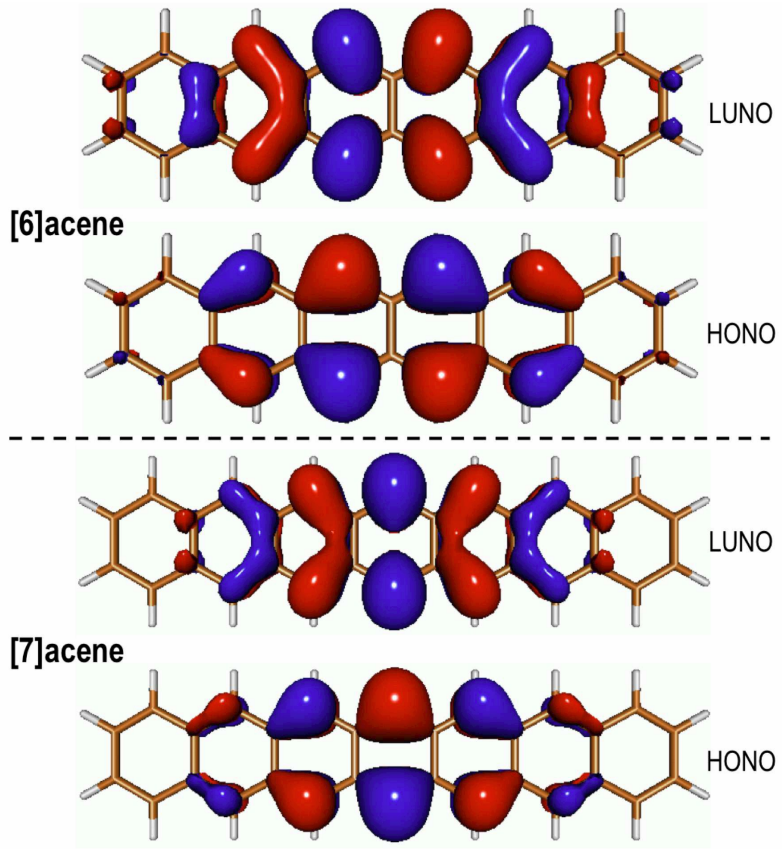

Figure 5: Plots of RAS-SF frontier natural orbitals for hexacene (top) and heptacene (bottom).

View Article Online
DOI: 10.1039/C8CP00135A

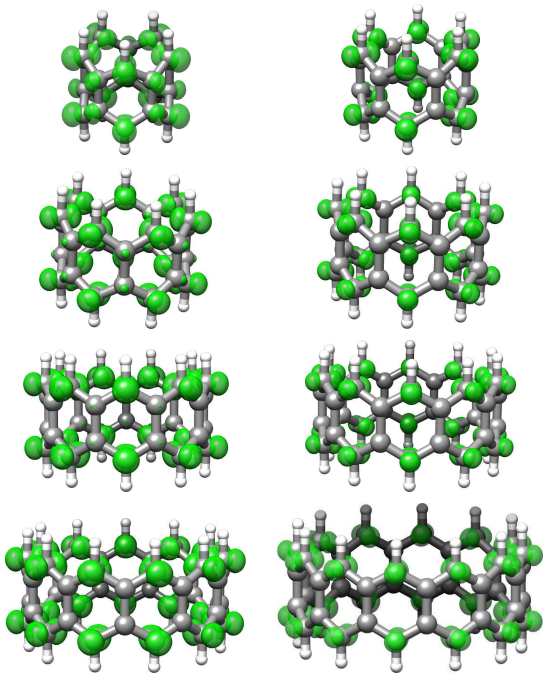

Figure 6: Plots of the FOD density ($\sigma = 0.005$ e/bohr^3) for $[n]$CCs of increasing size ($n = 5 - 12$), as obtained from the FT-DFT method.

View Article Online
DOI: 10.1039/C8CP00135A

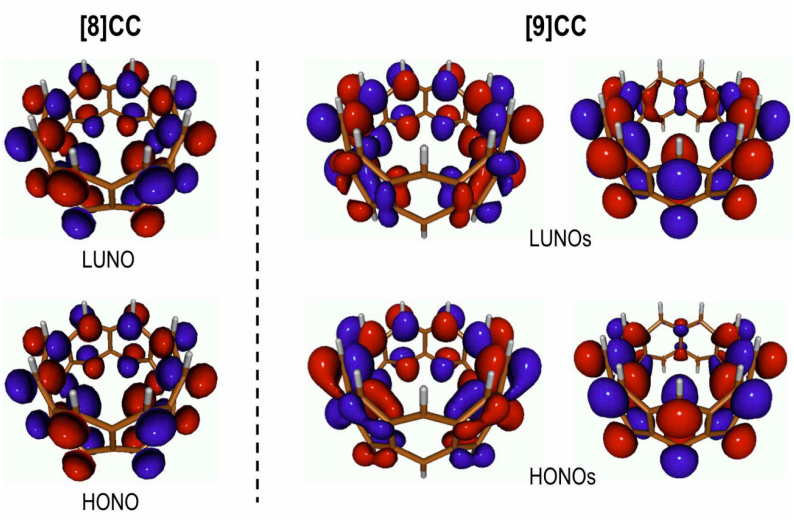

Figure 7: Plots of RAS-SF frontier natural orbitals for $[n]$CC with $n = 8$ (left) and $n = 9$ (right).

View Article Online
DOI: 10.1039/C8CP00135A

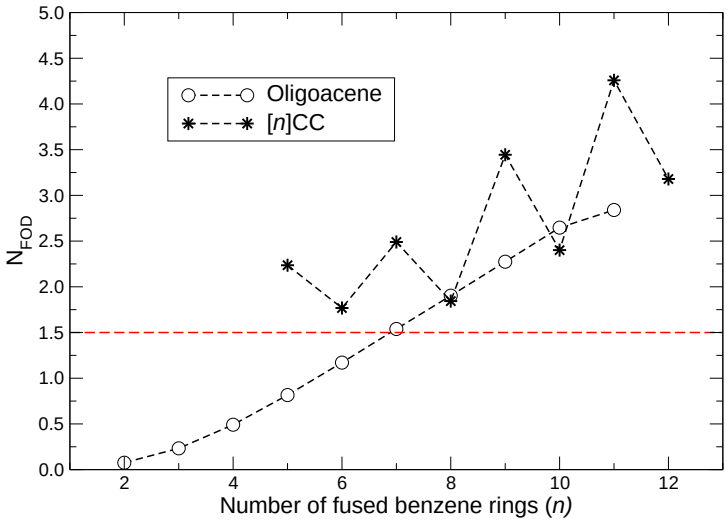

Figure 8: Evolution of the N_{FOD} values, as obtained from the FT-DFT method, as a function of the oligomer size for both linear and cyclic acenes. The dashed red line corresponds to $N_{FOD} = 1.5$.

View Article Online
DOI: 10.1039/C8CP00135A

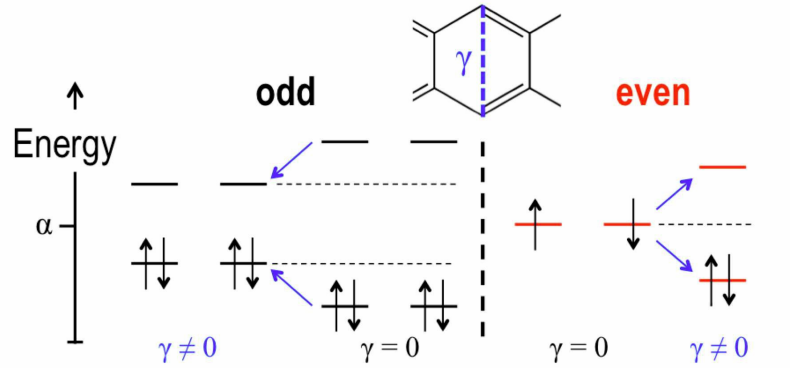

Figure 9: Effect of the radical center interaction (γ) in the Hückel frontier orbitals for [n]CC with n-odd (left) and n-even (right). Introduction of $\gamma \neq 0$ in linear acenes systematically reduces the HOMO-LUMO gaps.

View Article Online
DOI: 10.1039/C8CP00135A

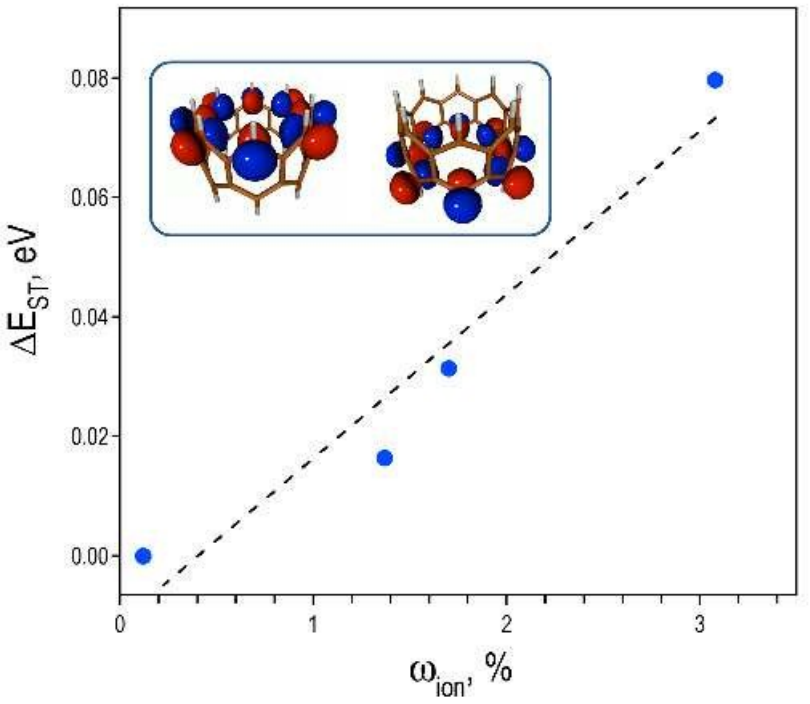

Figure 10: Correlation between ionic contributions ($\omega_{ion} = 100 \times |c_{ion}|^2$) and singlet-triplet energy gaps for the RAS-SF ground state wave functions of $[n]$CC molecules with n-even as indicated in Eq. (6). Note that values in the graph have to be considered only qualitatively since fragment decomposition has been done with a small active space (see Computational details). Inset shows fragment orbitals for the case with $n = 8$. Dashed line corresponds to the regression line only plotted for guidance.

View Article Online
DOI: 10.1039/C8CP00135A

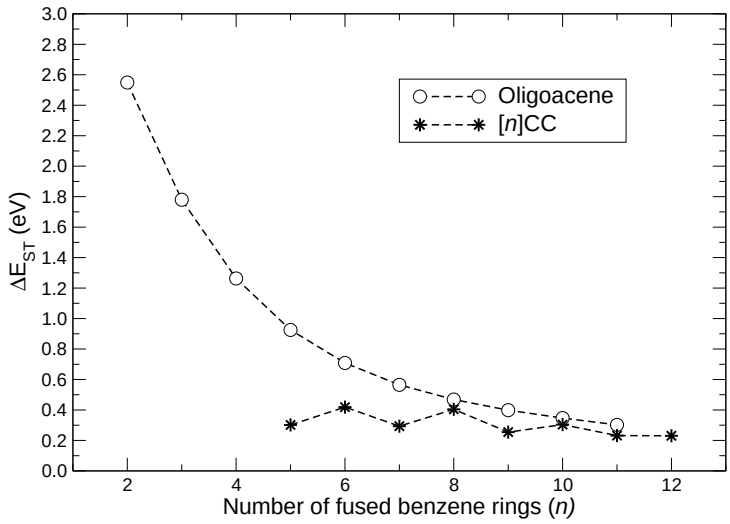

Figure 11: Evolution of the ΔE_{ST} values, as obtained from the FT-DFT method, as a function of the oligomer size for both linear and cylic acenes.

View Article Online
DOI: 10.1039/C8CP00135A

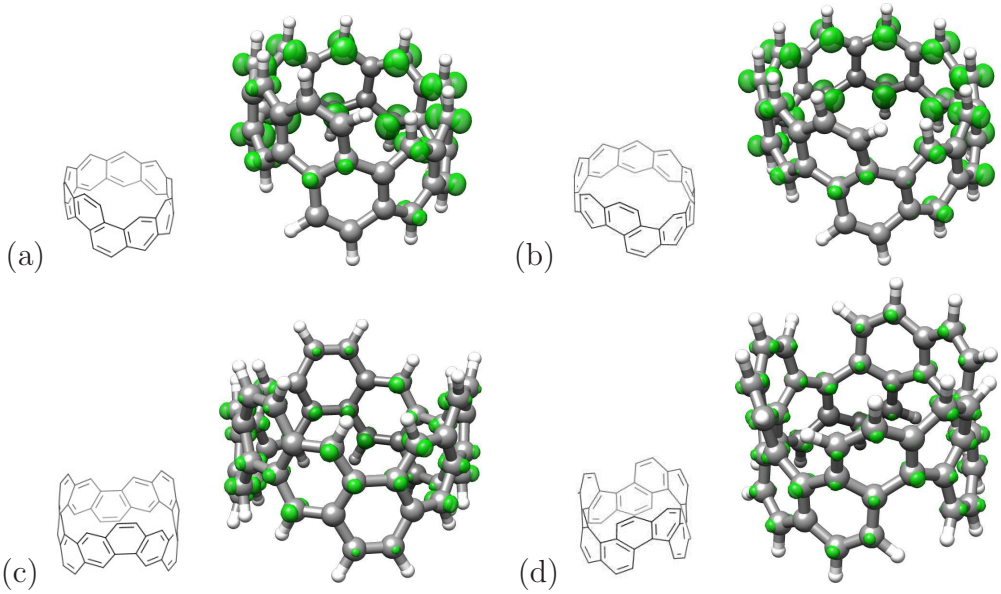

Figure 12: Chemical structures and plots of the FOD density, as obtained from the FT-DFT method, for: (a) cyclo[a]decacene ($\sigma = 0.005$ e/bohr^3), (b) cyclo[a]undecacene ($\sigma = 0.005$ e/bohr^3), (c) [3]cyclobenzo[a]anthracene ($\sigma = 0.002$ e/bohr^3), and (d) [3]cyclochrysene ($\sigma = 0.002$ e/bohr^3).

View Article Online
DOI: 10.1039/C8CP00135A

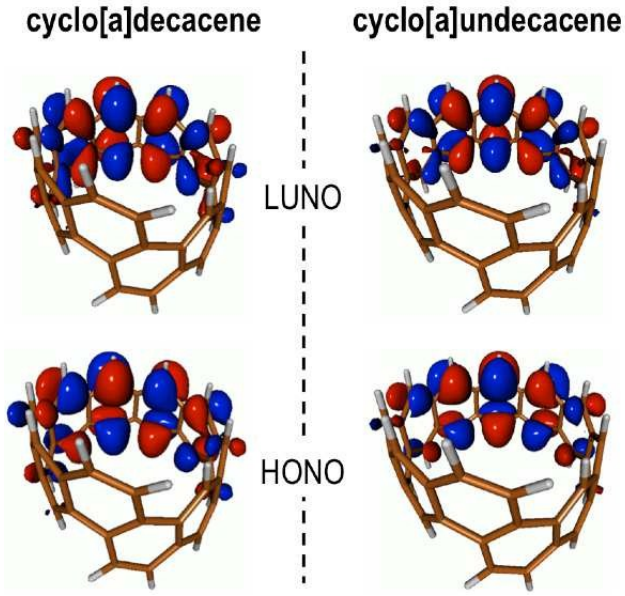

Figure 13: Plots of RAS-SF frontier natural orbitals for cyclo[a]decacene (left) and cyclo[a]undecacene (right).